Exploration of Graphene Layers in Various Carbon Materials by Raman Spectroscopic Techniques

Jelby George*, Shanyukta Upadhyay†

& Manoj Balachandran‡

Abstract

Structural figure prints for identifying the molecules in graphene layers of various carbon materials can be obtained from Raman spectroscopy. In this review we have discussed the Microraman analysis of few- layer graphenes from different carbon samples originating from hydrocarbon and agricultural derivatives. This review also shows the crystallite size dependence of the D-band in the Raman spectrum. Deconvolution of broad signal peaks is done to get multiple overlapping bands giving information about various aspects of defects and structure of graphitic materials. This review also contains information regarding different types of defects that can be analyzed using Raman spectroscopy.

* Department of Physics and Electronics, CHRIST (Deemed to be University), Bengaluru, Karnataka, India;
jelby.george@res.christuniversity.in
† Department of Physics and Electronics, CHRIST (Deemed to be University), Bengaluru, Karnataka, India;
shanyukta.upadhyay@christuniversity.in
‡ Department of Physics and Electronics, CHRIST (Deemed to be University), Bengaluru, Karnataka, India;
manoj.b@christuniversity.in

1. Introduction

Soot, a solid black product, is obtained from the partial combustion or pyrolysis of organic materials like fossil fuels. While this material has essential roles in industry as filler and pigment (carbon black), it is also a significant cause of pollution (diesel soot). The soot is primarily composed of more than 80% of carbon and contains clusters of primary particles with sizes ranging from 10 nm to 30 nm in both amorphous and crystalline states. The crystalline domains similar to graphite that are considered graphitic lattices with the high disorder are made of 3-4 graphene layers turbostratically stacked with a mean La (lateral extension) in the order of 3 nm and an interlayer separation of about 0.335 nm[1-3]. Parallel graphene layers in an ideal graphitic lattice have an alternating ABAB sequential arrangement with a separation of about 3.35 nm, indicating a hexagonal closest crystal structure. In the arrangement, lattice sites of two different types, having different coordination numbers hold unit cells of four carbon atoms. Two carbon atoms or none will be present on an axis perpendicular to the parallel layers. Amorphous non-graphite-like layer states are mostly made from graphene layer precursors like polycyclic aromatic compounds used in irregular arrangements such as fullernoids and other inorganic and organic components like sulfates, aliphatics, and metal oxides. Starting materials and the processing environment for combustion or pyrolysis affect the physical and chemical structure, elemental composition, and crystalline graphitic to amorphous (organic carbon) ratio of the soot [3-6]. Diffraction techniques are effective for the structural analysis of materials with long-range crystalline order.

Meanwhile, Raman spectroscopy has more potential when it comes to the case of highly disordered materials like soot. Besides the crystal structure, Raman spectroscopy focuses on parameters in short-range order, like molecular structures. The Raman spectra of graphite crystals are attributed to the lattice vibrations and can effectively sense the extent of structural disorder. Distorted graphitic lattices, like regular graphite (polycrystalline) or boron-doted HOPG, show a significant difference in the Raman spectrum compared to near-ideal graphite, obtained from highly oriented polycrystalline graphite (HOPG)[6-11] and large single graphitic crystals.

Different types of graphitic materials [1,12-14] like diamond films, glassy carbon[15], coal fibers[11,16], amorphous and graphitic carbon films, coal, fullerenes[11], and activated carbon were investigated by various groups. Some studies say that degree of graphitization can be used to distinguish between various types of soots, using various approaches for study and analysis of the wide and conjoining Raman bands. Differences in methods used for determining spectral parameters related to the degree of graphitization make the comparison of results hard and limit their conclusiveness. This scenario makes it relevant to examine the possibility of using Raman micro-spectroscopy to analyze the structure of soot materials by experimentation and spectroscopic studies. Under distinct conditions, the Raman spectra of a wide variety of soot and related materials were recorded with a Raman microscope system (excitation wavelengths ranging from 514nm to 1064nm). Further studies of the obtained spectral data are done using curve fitting of various band combinations. A reflection on the structural analysis and significance of spectral parameters is done on account of the outcomes of earlier reported works. Micro-Raman analysis of graphene-like structure derived from soot.

Raman spectroscopy plays a crucial role in clarifying the of structure of graphite-based materials as it provides pretty relevant information regarding, graphene layers and their stacking, crystallite size, and especially defects present in the material. Raman spectroscopy is one of the best tools to characterize hybridization of carbon atoms (sp2 and sp3) present in graphite, poly-aromatic compounds, diamond, coal, and other allotropes of carbon[17].

The first-order Raman spectral band (G band) of pure graphite (Fig 1) was observed at ~ 1580 cm-1 and is attributed to an ideal lattice vibration mode with E2g symmetry. The intensity of the first-order defect band (D) observed in the spectrum due to characteristic disordered graphite shoots up with an increase in disordered graphitic structures. At 1350 cm-1, the D1 band is present, which is the most intense among the others, and it tells us about the vibration mode of graphitic lattice and A1g symmetry. Similarly, one more band (D2) is observed at 1606 cm-1 as a shoulder of the G

band, which is attributed to E2g symmetry for graphitic lattice mode.
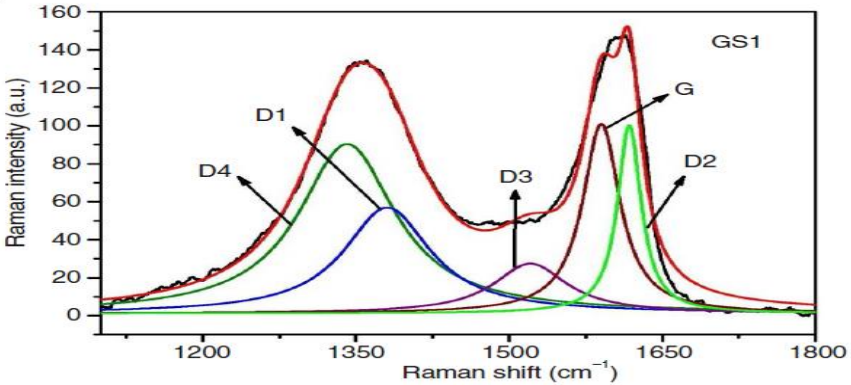
Fig. 1: Deconvoluted first-order Raman spectrum for intercalated graphite.

Only some vibrational modes are Raman active[1,18-19] for an ideal graphitic crystal. As discussed in the review, several research groups have investigated Raman fingerprints for single and few-layered graphene. Micro Raman spectra of samples derived from Kerosene (KS), camphor (CS), and the samples treated by Hummer's method (KS1 and CS1) are presented in figures 2(a) and (b). The peak observed at 1583 cm-1 gives information about the presence of first order mode for graphite-like structure (G-peak) with high frequency (E2g). D peak centered around 1350 cm-1 shows defects present within the crystal structure. The intensity ratio ID/IG (defect to graphitic peak ratio) is 0.82, 0.91, 0.95 and 0.98 for the following samples KS, KS1, CS and CS1 and the results are similar to other outcomes reported on graphite and grapheme[19-22].
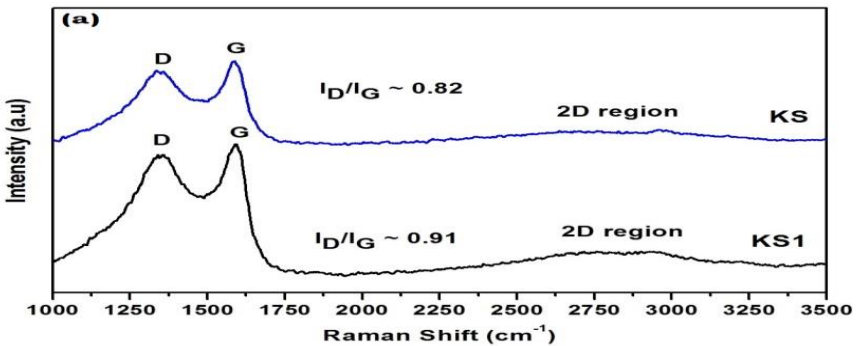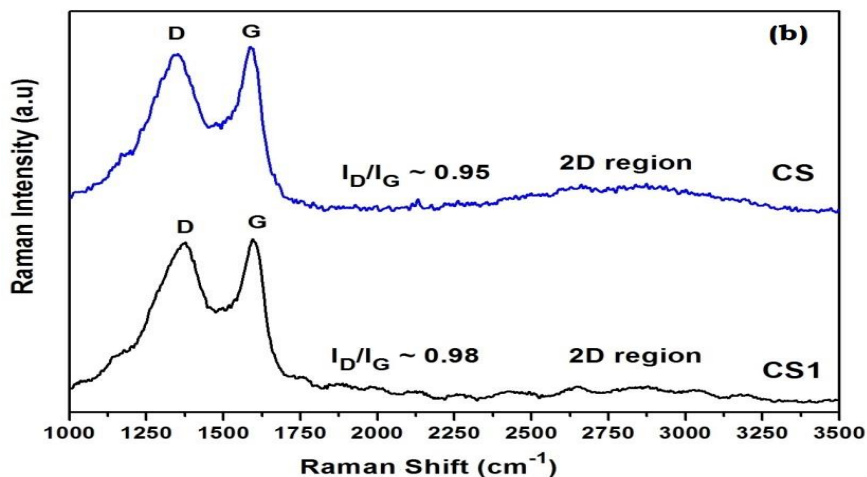
Fig.2: (a) Raman analysis of KS sample (b) Raman analysis of CS sample.

It is evident that the defect ratio changes or more defects are introduced to the graphitic plane with Hummer's treatment. It also reflects that more functional groups are attached to the graphitic plane. Some reports show that with an increase in the number of layers, the G band's intensity also increases considerably, whereas that of the 2D band decreases [20]. To determine the spectral parameters by fitting, several combinations for Raman bands (first order) have been used, and It is observed that almost five bands (G, D1, D2, D3 & D4) are there for the first order.

Earlier studies on Raman spectra of soot used to consider G, D & D3 bands. D3 band present at 1500cm-1 starts from the unstructured carbon part of soot which includes organic molecules or functional groups. Unstructured carbon allocation over the interstitial sites for the disordered graphitic lattice of soot led Jwhari et al.[21] To project a gaussian type shape for this band. Spectral analysis is shown here to support the output. Unlike the band combinations used in many earlier studies, this grouping permitted us to explain all spectra measured with quite compatible goodness-of-fit. With the knowledge of spectral parameters of the corresponding bands, we can explain the dependence of excitation wavelength of laser and it is also possible to distinguish between diverse sample materials. There is still a significant amount of statistical uncertainty after the deconvolution of several highly overlapping bands. For similar soot spectra, spectral parameters are

highly variable. D4 band appears as a shoulder peak (~1200 cm-1) to the peak at ~1350 cm-1.[24] Sadesky et al. have shown a Lorentzian shape near ~1180 cm-1 for certain soot samples[1]. For C-C and C=C stretching or sp2-sp3 bonds vibrations of polyene-like structures, a band is observed at around 1190 cm-1 for the Raman spectra of flame soot. In figure 3, at positions ~2450 cm-1, 2700 cm-1, and 3250 cm-1, second-order bands of Raman spectra can be seen clearly, similar to those present in the spectrum of graphite. It confirms the formation of graphite-like carbon in soot. G band observed is highly intense in comparison to the 2D band. The 2D band is further fitted with several Lorentzian profiles with four peaks corresponding to G*, G′, D+D′ and 2D′ bands.

This band splitting is ascribed to the splitting of π electron dispersion energies present due to   the interaction between neighboring graphitic planes[22].
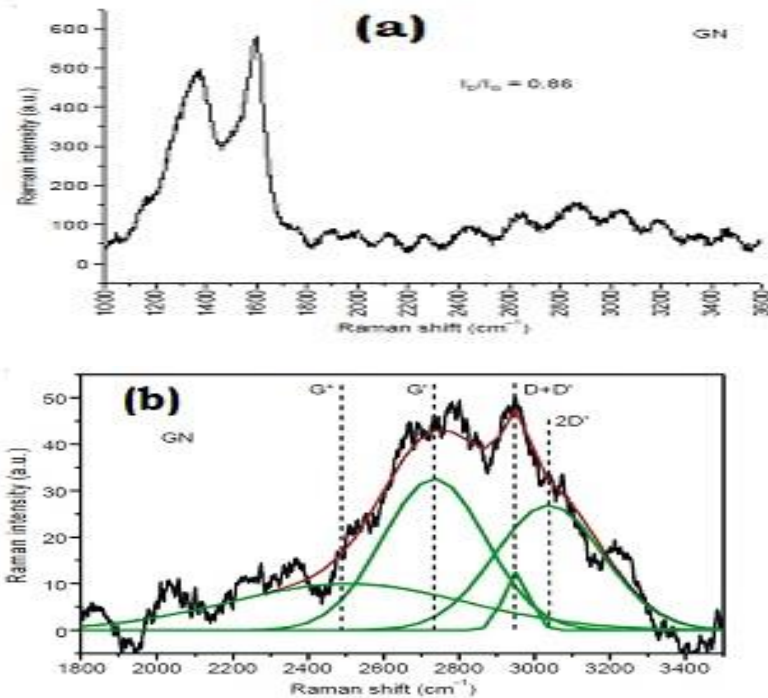
Fig. 3: (a) Raman spectrum of sub-bituminous coal (GN-leached with *Aspergillus niger*) (b) Fitting of curve for the second order Raman spectrum of sub-bituminous coal (GN).

Furthermore, this band also belongs to the D band's overtone and can be attributed to disorder induced in the graphene layers. G' band's location depends on stacking order and the number of layers of the graphite sample. One can identify i any modification done in the graphite-based lattice by analyzing the G* and G' bands. The two peak profile for 6-8 layers of graphene layers piled in proper order is exhibited by the G' peak (2D peak).

In samples with larger c-axis disorder, the two peak profile of graphite is not retained. With increment in disorders, there is an upward shift in the G' shoulder peak, which further results in a single 2D band (G' band). The reason for this is the 3 dimensional graphitic structure and the turbostraticity.. Figure 4 shows samples treated by modified Hummers' method, CSS (coconut shell) and WS (wood) reveals two profiles in the 2D region which confirms the formation of a few layers of graphitic structure[23-25].
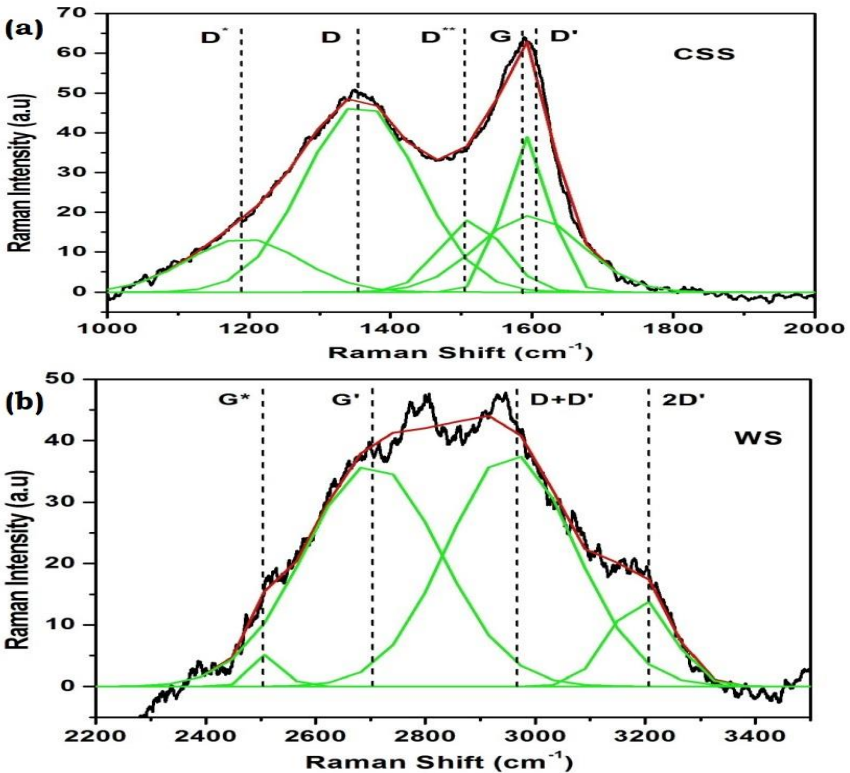
Fig.4: Spectral analysis of (a) CSS sample (b)WS sample.

Due to disorders in the structure, some otherwise restricted vibrational modes formed become Raman Active. In carbonaceous materials (polycrystalline) that contain many small graphitic crystallites, the D band is considered to have originated from the carbon atoms that hold the edge positions of the graphene layers. Among the Raman Spectral bands (second-order) present at ~2450 cm-1, 2700 cm-1, and 3250 cm-1, the band present at 2720 cm-1 and 3250 cm-1 denote the first overtones of D1 and D2 bands, respectively. An absorption peak seen at 2450 cm-1 is attributed to the first overtone (Raman active) of a graphitic lattice vibration mode (~1200 cm-1) that is Raman-inactive.

The Raman spectra of soots prepared from kerosene, diesel, and carbon black at 514 nm excitation wavelength was deconvoluted to understand the characteristics related to its carbon constituents. Five bands were clearly distinguished in the first-order spectrum after deconvolution, as seen in figure 5. The G peak (1585 cm-1) has an additional D2 band due to the graphitic-like planes. The D3 band, at ~1500 cm-1, originates from the amorphous part of the soot. D1 and D4 peaks at 1350 cm-1 and about 1200 cm-1, respectively, appear due to the presence of the sp2-sp3 hybridized mixed phase of the carbon[18].
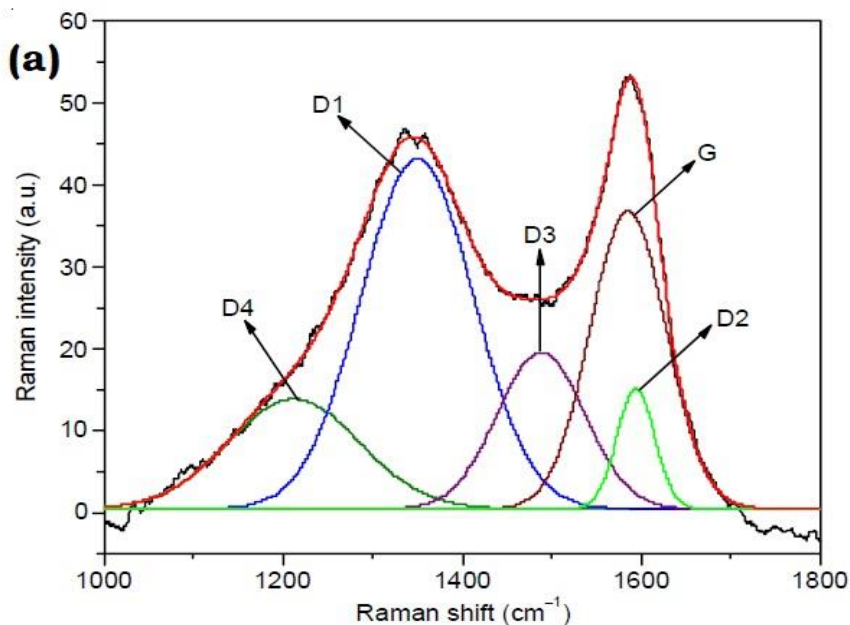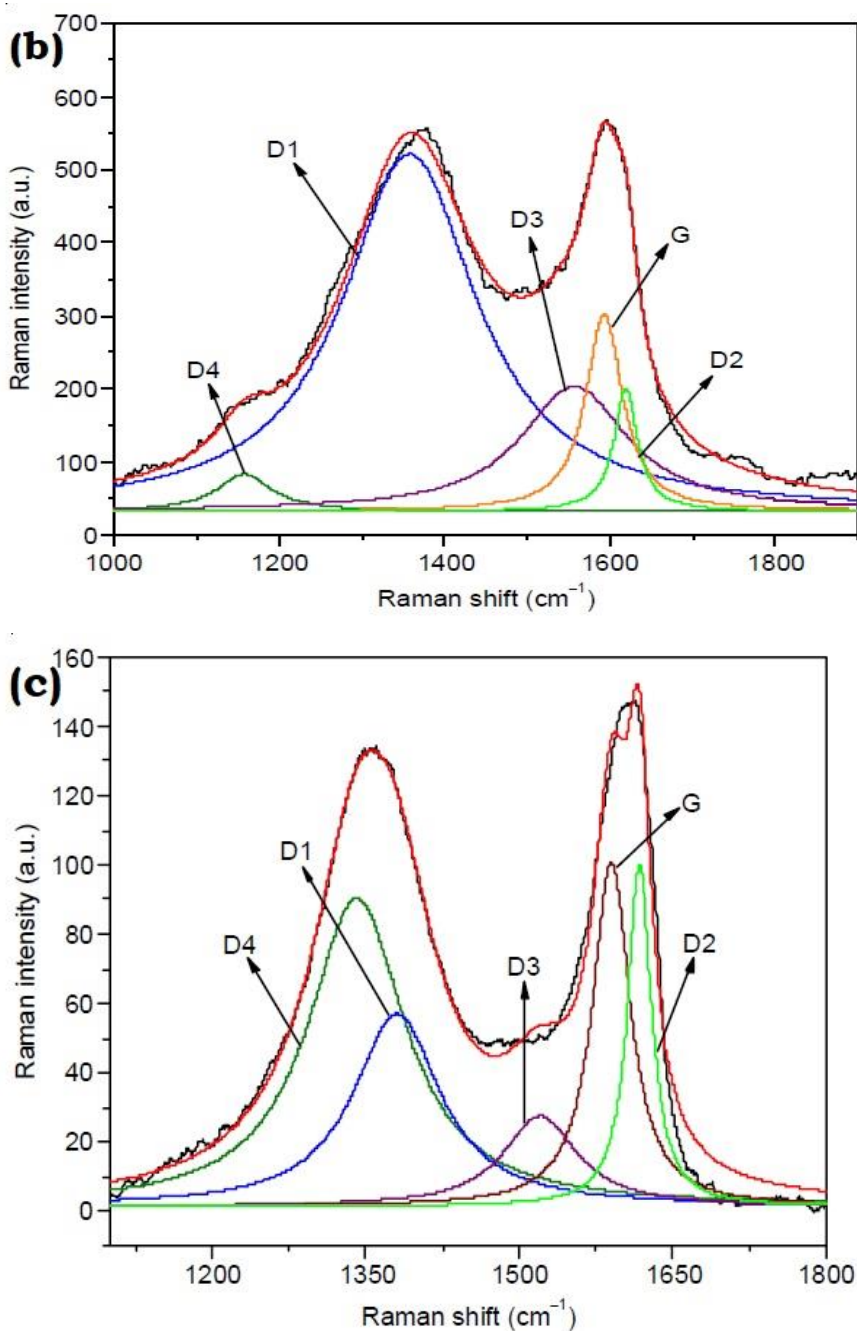
Fig.5: (a) Spectral analysis of (kerosene soot) KS1 sample
    (b) Spectral analysis of diesel soot
    (c) Spectral analysis of carbon black soot. Reprinted with permission from [18]

Investigating the characteristics of G, D and 2D-bands is necessary to understand the disordered carbon structure. The occurrence of the G-band is attributed to the bonded carbon (sp2) in the hexagonal graphitic planes. At the same time, the D' band is due to peaks near the high-frequency edge related to the vibrational density of states (DOS) of the carbon lattice [1-2], which becomes Raman active with the break down of the k=0 selection rule. Hence, as a result of Raman scattering, the inner graphitic plane is responsible for the G-band in the spectrum. The 2D band is the overtone of the D band, and it is strongest when the graphitic structure is highly ordered. For carbon with a high degree of order, this band is generally present at 2607 cm-1, and it shifts towards smaller wavenumbers as the disorder increases.

2. Crystallite size dependence of the D-band

Tuinstra and Koenig [8] developed a methodical study of Raman and X-ray diffraction results from many graphitic samples with various in-plane crystallite sizes La. They concluded that ID/IG is inversely proportional to La for naono crystalline substances as shown in figure 6.
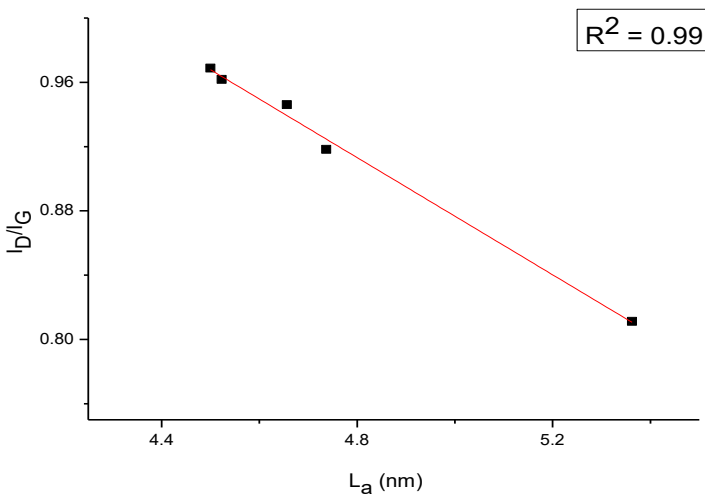
Fig. 6: Plot shows ID/IG versus La.

3. Defect analysis Using Raman spectroscopy

In 1970, Tuinstra and Koenig introduced Raman spectral analysis of graphite. The spectrum of graphitic single crystals shows a maximum point at 1575 cm-1 which corresponds to the E2g phonon mode in-plane vibrations of the G peak. Raman spectrum of some graphitic materials like carbon black, vitreous carbon and activated charcoal shows an extra peak at ~1355 cm-1, resulting from the A1g breathing modes at the Brillouin zone. The intensity of the peak mentioned above increases from pyrolitic graphite (stress annealed) to commercial graphite and further to carbon black with the increase in the number of un-ordered carbon and reduction in crystal size of the graphite. Hence, any distortion in the graphene lattice symmetry can be observed through D-peak. Both G and D bands play a crucial role in explaining the degree of disorderliness in the system. In particular, no D-band peak is observed in pure graphite but additional defect peaks are observed in disordered systems[24-26]. These defect peaks give relevant information about the nature of the disorder[27-33].

Sadezky et.al., (2005) [1] has reported the Raman spectrum of several carbon-based samples, such as diesel soot and carbon black, divided into two spectra. The first spectrum can be deconvoluted into five bands: G, D1, D2, D3, and D4 at 1575cm-1, 1360 cm-1, 1620cm-1, and 1500cm-1, 1180cm-1, respectively. Among these, the G peak is related to graphitic order, while the D peak refers to defect-originated peaks. The other spectrum is called second-order spectrum, deconvoluted into several main peaks named G*, 2D or G′, D+D′ and 2D′(G′′) bands 2450cm-1, 2700cm-1 2950cm-1, 3250cm-1 respectively. Among these peaks, the 2D band forms the first overtone of the D1 band. The fewer graphene layers, the sharper the peak will be. Therefore single-layer graphene peak is the sharpest. Different types of disorders with corresponding defect peaks are shown in table 1. Hence, the deconvolution of both first and second order Raman spectrum shows the involvement of all defect-generated peaks and graphitic peaks(G).

**Table 1: Types of disorders and its associated peak positions.
Data taken with permission from [30].**

Sl.No	Order of Spectra	Band Name	Position (cm-1)	Type of disorder	Reference
1	First Order	D or D1	1360	structural disorder/ heteroatom /doped graphene	[1][30]
2		D′ or D2	1620	point defects	[26][30]
3		D3 or D**	1500	interstitial defects/ amorphous carbon	[1][27][30]
4		D4 or D*	1180	sp2 – sp3 hybridised atoms	[1][30]
5	Second Order	D+G or D+D′	2950	ion implantatio n	[28]

Therefore table 1 shows that the first order D or D1 peak corresponds to the structural disorder of the doped graphene and that the D′ peak shows the point defects and is observed as a shoulder peak in G. To find the degree of disorderliness in the sample, I_D/I_G can be calculated. Similarly, the $I_D/I_{D'}$ ratio can be used to find the specific nature of the point defect, as presented in table 2. On-site defects arise from the out-of-plane atoms bonded to carbon atoms, whereas the deformation in the carbon bond leads to hopping defects[27-30,34].

Table 2: Nature of defects and their corresponding ID/ID' ratio. Data taken with permission from [30]

Sl.No	Nature of defects	$I_D/I_{D'}$
1	Single vacancy	1
2	Double vacancy	11
3	Stone-Wales	17
4	sp^3	13
5	Grain Boundaries	3.5
6	Hopping defects	10.5
7	On-site defects	1.3

With an increase in the degree of disorder, the FWHM of respective peaks becomes wider with sharp intensity, which explains the shape dependence of Raman spectra on defects density[32]. Increment in FWHM of G peak, with a constant D peak also refers to certain disorders. Doping effects can be observed in the 2D overtone peak, almost four times stronger than G peak for low doping. Highly broadened G and D bands may correspond to wrinkles in graphene with a shifted bump in the 2D band [19, 27-28, 32-36].

4. Conclusion

Analysis of the Raman spectrum of graphitic structures gives insight into its structural arrangements, defects and degree of disorder. The spectral analysis justified the presence of five bands in the first-order spectral region after curve fitting. The second-order Raman spectrum gives information about the number of layers in several soot materials derived from various precursors. The obtained spectra are deconvoluted to study different types of bands. We have also explained the dependence of different defects on the ID/ID' ratio calculated from the Raman spectra.

References

[1] Sadezky A et al., Raman microspectroscopy of soot and related carbonaceous materials: spectral analysis and structural information, Carbon 43(2005), 1731-1742.

[2] Lahaye J, Prado G. In: Thrower PA, editor. Chemistry and physics of carbon, vol. 14. New York: Decker; 1978. p. 14. 168.

[3] Homann K H. Fullerenes and soot formation—new pathways to large particles in flames. Angew Chem Int Ed 1998; 37:2434–51.

[4] Dippel B, Heintzenberg J. Soot characterisation in atmospheric particles from different sources by NIR FT Raman spectroscopy. J Aerosol Sci 1999; 30(Suppl. 1): 907–8.

[5] Ramsteiner M, Wagner J. Resonant Raman scattering of hydrogenated amorphous carbon: evidence for p-bonded carbon clusters. Appl Phys Lett 1987; 51:1355–7.

[6] Gruber T, Waldeck-Zerda T, Gerspacher M. Raman studies of heat-treated carbon blacks. Carbon 1994; 32:1377–82.

[7] Nakamizo M, Honda H, Inagaki M, Hishiyama Y. Raman spectra, effective Debye parameter and magnetoresistance of graphitized cokes. Carbon 1977; 15:295–8.

[8] Tuinstra F, Koenig J L. Raman spectrum of graphite. J Chem Phys 1970; 53:1126–30.

[9] Nemanich R J, Solin S A. First-and second-order Raman scattering from finite-size crystals of graphite. Phys Rev B 1979;20:392–401.

[10]Al-Jishi R, Dresselhaus G. Lattice-dynamical model for graphite. Phys Rev B 1982; 26:4514–22.

[11]Dresselhaus M, Dresselhaus S G. Intercalation compounds of graphite. Adv Phys 1981; 30:290–8.

[12]Wang Y, Alsmeyer D C, McCreery R L. Raman spectroscopy of carbon materials: structural basis of observed spectra. Chem Mater 1990; 2:557–63.

[13] Cuesta A, Dhamelincourt P, Laureyns J, Martinez-Alonso A, Tascon J M D. Raman microprobe studies on carbon materials. Carbon 1994; 32:1523–32.

[14] Sze S K, Siddique N, Sloan J J, Escribano R. Raman spectroscopic characterization of carbonaceous aerosol. Atmos Environ 2001; 35:561–8

[15] Nakamizo M, Kammereck R, Walker Jr PL. Laser Raman studies on carbons. Carbon 1974; 12:259–67.

[16] Manoj B and Kunjomana A G, FT-Raman Spectroscopic study of Indian Bituminous and Sub-bituminous coal, Asian Journal of Material Science 2(4) (2010) 204-210.

[17] Manoj, B. "Bio-demineralization of Indian bituminous coal by Aspergillus niger and characterization of the products." Research Journal of Biotechnology 8.3 (2013): 49-54.

[18] Mohan, Anu N., B. Manoj, and A. V. Ramya. "Probing the nature of defects of graphene like nano-carbon from amorphous materials by Raman spectroscopy." Asian Journal of Chemistry 28.7 (2016): 1501.

[19] Elcey, C. D., and B. Manoj. "Graphitization of coal by bio-solubilization: structure probe by Raman spectroscopy." Asian Journal of Chemistry 28.7 (2016): 1557.

[20] AM Raj, M Balachandran "Coal-Based Fluorescent Zero-Dimensional Carbon Nanomaterials: A Short Review", Energy & Fuels 34 (11), 13291-13306

[21] Jawhari, T., A. Roid, and J. Casado. "Raman spectroscopic characterization of some commercially available carbon black materials." Carbon 33.11 (1995): 1561-1565.

[22] Jiang, Jie, et al. "A Raman spectroscopy signature for characterizing defective single-layer graphene: Defect-induced I (D)/I (D′) intensity ratio by theoretical analysis." Carbon 90 (2015): 53-62.

[23] Manoj B, Ashlin M Raj, George Thomas C. Tailoring of low grade coal to fluorescent nanocarbon structures and their potential as a glucose sensor. Scientific reports 8 (1) (2018), 1-9.

[24] Dresselhaus, M. S., et al. "Defect characterization in graphene and carbon nanotubes using Raman spectroscopy." Philosophical Transactions of the Royal Society A: Mathematical, Physical and Engineering Sciences 368.1932 (2010): 5355-5377.

[25] Whelan, Paul. Raman microscopy studies of carbon particles from diesel particulate matter (DPM) and coal dust. Sheffield Hallam University (United Kingdom), 2001.

[26] Ferreira, E H Martins, et al. "Evolution of the Raman spectra from single-, few-, and many-layer graphene with increasing disorder." Physical Review B 82.12 (2010): 125429.

[27] Ferrari, Andrea C., and John Robertson. "Interpretation of Raman spectra of disordered and amorphous carbon." Physical review B 61.20 (2000): 14095.

[28] Wang, Yan, Daniel C. Alsmeyer, and Richard L. McCreery. "Raman spectroscopy of carbon materials: structural basis of observed spectra." Chemistry of Materials 2.5 (1990): 557-563.

[29] Manoj B, Elcey C D "Demineralization of coal by stepwise bioleaching: a study of sub-bituminous Indian coal by FTIR and SEM" Journal of the University of Chemical Technology and metallurgy 45 (4),(2010) 385-390.

[30] Mathew, Elma Elizaba, and B. Manoj. "Disorders in graphene: types, effects and control techniques—a review." Carbon Letters (2021): 1-20.

[31] Wu, Zhangting, and Zhenhua Ni. "Spectroscopic investigation of defects in two-dimensional materials." Nanophotonics 6.6 (2017): 1219-1237.

[32] Jiang, Jie, et al. "A Raman spectroscopy signature for characterizing defective single-layer graphene: Defect-induced I (D)/I (D′) intensity ratio by theoretical analysis." Carbon 90 (2015): 53-62.

[33] Manoj, B. "Synthesis and characterization of porous, mixed phase, wrinkled, few layer graphene like nanocarbon from charcoal." Russian Journal of Physical Chemistry A 89.13 (2015): 2438-2442.

[34] Ramya, Krishnan, Jerin John, and B. Manoj. "Raman
     spectroscopy investigation of camphor soot: spectral analysis
     and structural information." Int. J. Electrochem. Sci 8 (2013):
     9421-9428.

[35] Mathew, Elma Elizaba, and Manoj Balachandran. Crumpled
     and porous graphene for supercapacitor applications: a short
     review." Carbon Letters, 31(2021): 537–555.

[36] Ramya AV, Anu N Mohan, and Manoj Balachandran.
     "Wrinkled graphene: synthesis and characterization of few
     layer graphene-like nanocarbons from keroscene" Materials
     Science-Poland. 34(2), (2016): 330-336.